Published in final edited form as:
Br J Ophthalmol. 2009 August ; 93(8): 1057–1063. doi:10.1136/bjo.2009.157875.

Retinal nerve fibre layer thickness measurement reproducibility improved with spectral domain optical coherence tomography

J S Kim[1,2], **H Ishikawa**[1,2], **K R Sung**[1], **J Xu**[1], **G Wollstein**[1], **R A Bilonick**[1], **M L Gabriele**[1], **L Kagemann**[1,2], **J S Duker**[3], **J G Fujimoto**[4], and **J S Schuman**[1,2]

[1]UPMC Eye Center, Eye and Ear Institute, Ophthalmology and Visual Science Research Center, Department of Ophthalmology, University of Pittsburgh School of Medicine, Pittsburgh, Pennsylvania, USA

[2]Department of Bioengineering, Swanson School of Engineering, University of Pittsburgh, Pittsburgh, Pennsylvania, USA

[3]New England Eye Center, Tufts Medical Center, Boston, Massachusetts, USA

[4]Department of Electrical Engineering and Computer Science and Research Laboratory of Electronics, Massachusetts Institute of Technology, Cambridge, Massachusetts, USA

Abstract

Background/aims—To investigate retinal nerve fibre layer (RNFL) thickness measurement reproducibility using conventional time-domain optical coherence tomography (TD-OCT) and spectral-domain OCT (SD-OCT), and to evaluate two methods defining the optic nerve head (ONH) centring: Centred Each Time (CET) vs Centred Once (CO), in terms of RNFL thickness measurement variability on SD-OCT.

Methods—Twenty-seven eyes (14 healthy subjects) had three circumpapillary scans with TD-OCT and three raster scans (three-dimensional or 3D image data) around ONH with SD-OCT. SD-OCT images were analysed in two ways: (1) CET: ONH centre was defined on each image separately and (2) CO: ONH centre was defined on one image and exported to other images after scan registration. After defining the ONH centre, a 3.4 mm diameter virtual circular OCT was resampled on SD-OCT images to mimic the conventional circumpapillary RNFL thickness measurements taken with TD-OCT.

Results—CET and CO showed statistically significantly better reproducibility than TD-OCT except for 11:00 with CET. CET and CO methods showed similar reproducibility.

Conclusions—SD-OCT 3D cube data generally showed better RNFL measurement reproducibility than TD-OCT. The choice of ONH centring methods did not affect RNFL measurement reproducibility.

Correspondence to: Dr G Wollstein, UPMC Eye Center, Department of Ophthalmology, University of Pittsburgh School of Medicine, 203 Lothrop Street, Eye and Ear Institute, Suite 834, Pittsburgh, PA 15213, USA; wollsteing@upmc.edu.
JSK and HI contributed equally.

Competing interests: JGF and JSS receive royalties for intellectual property licensed by Massachusetts Institute of Technology to Carl Zeiss Meditec. JGF is a scientific advisor and has stock options with Optovue. GW received research funding from Carl Zeiss Meditec and Optovue. HI, GW and JSS receive royalties for intellectual property, licensed by University of Pittsburgh to Bioptigen, Inc.

Ethics approval: Ethics approval was provided by the institutional review board at the University of Pittsburgh.

Patient consent: Obtained.

Presented in part at the annual meeting of the Association for Research in Vision and Ophthalmology, Fort Lauderdale, Florida, April 2008.

Retinal nerve fibre layer (RNFL) thickness measurement has become a widely employed clinical technique for glaucoma assessment.[1–3] Optical coherence tomography (OCT) is a technology providing RNFL thickness measurements in a non-contact and non-invasive fashion.[4 5] RNFL thickness is measured on a cross-sectional retinal image sampled along a 3.4 mm circle centred to optic nerve head (ONH).[6] Due to the relatively slow axial scan rate of standard time-domain OCT (TD-OCT, 400 axial scans per second, or ~0.64 s scanning for 256 axial scans per circle used in Stratus OCT (Carl Zeiss Meditec, Dublin, California)), the actual OCT axial scans may occur in the vicinity of the planned scanning path—a 3.4 mm circle around the ONH—jittering due to eye motion, one of the major sources of measurement variability (fig 1A, left). In order to minimise the influence of eye motion, three consecutive circular OCT scans are performed, and the mean RNFL thickness is computed after obtaining the measurements on each circular scan.[7] Another source of variability is scan circle placement. This affects where the OCT scan is projected onto retina (fig 1A, right). Since circle placement is manually controlled, it is difficult to ensure consistent image sampling location.

The recent introduction of spectral domain OCT (SD-OCT) has improved the scanning speed (60–100× faster, or 24 000–55 000 axial scans per second) and axial resolution (3.5–8 μm vs 8–10 μm with conventional TD-OCT) enabling high-resolution, three-dimensional (3D) volume sampling.[8–11] By performing a raster scan to acquire a volumetric data set and summing the back scattered signal at each transverse point on the retina, 3D SD-OCT data can be visualised as an en face image of the scanned area on the retina, which is called an OCT fundus image (fig 1B, upper).[10 12] The OCT fundus image allows us to detect eye motion during scanning by checking the retinal blood vessel integrity (fig 1B, lower).

Commercial SD-OCT (Cirrus HD-OCT; Carl Zeiss Meditec; software version: 3.0) acquires a volumetric data set and uses software to detect the ONH margin automatically on the OCT fundus image and calculate the geometric centre of a given ONH. Then, it resamples the 3D OCT data to generate a virtual 3.4 mm circular scan mimicking the conventional peripapillary OCT scan in order to maintain backward data comparability. With this fully automated RNFL thickness measurement method, the previously mentioned image registration limitation due to eye motion should be reduced. With these advantages, we hypothesise that SD-OCT shows a lower RNFL thickness measurement variability than conventional TD-OCT.

Fully automated SD-OCT measurements may still not be perfect, however, because no single OCT fundus image is identical to others. In other words, factors like minor eye motion during scanning, head position and a slight shift of subjects' fixation points may distort the OCT fundus image very slightly, but enough to be detected when superimposed onto other OCT fundus images (fig 2). In the past, scanning laser ophthalmoscope (SLO; Heidelberg Retina Tomography (HRT), Heidelberg Engineering, Heidelberg, Germany) exhibited a similar registration problem. Their solution for this problem was to import the ONH margin from the baseline image onto other images so that multiple scans share one universal ONH margin minimising scan-to-scan sampling variability.

Cirrus software does not import the ONH margin information from one scan to another, but it may be advantageous to share one universal ONH margin as the HRT does in order to minimise RNFL measurement variability. The purpose of this study was (1) to compare RNFL thickness measurement reproducibility between TD-OCT and SD-OCT and (2) to evaluate the performance of centring the ONH each time (Centred Each Time (CET)) or using one universal ONH centre (Centred Once (CO)) among repetitive scans, in terms of RNFL thickness measurement reproducibility.

METHODS

Twenty-seven eyes of 14 healthy subjects from the University of Pittsburgh Medical Center Eye Center were enrolled. Eyes with no history or evidence of intraocular surgery, retinal disease or glaucoma, refractive error less than 8 D and normal-appearing ONHs qualified as normal healthy subjects.

All eyes showed normal comprehensive ocular examination and automated perimetry with glaucoma hemifield test (GHT) within normal limits (Humphrey Field Analyzer, Carl Zeiss Meditec). The peripapillary region was scanned on all eyes using conventional OCT (Stratus OCT) and SD-OCT (Cirrus) at the same visit. All scans were performed through undilated pupils. Institutional review board and ethics committee approval were obtained for the study, and informed consent was obtained from all subjects. This study followed the tenets of the Declaration of Helsinki and was conducted in compliance with the Health Insurance Portability and Accountability Act.

Image acquisition

Stratus OCT—Circular scans centred on the ONH were obtained using the "Fast RNFL Scan" pattern, which performs three 3.4 mm diameter circular scans (with 256 A-scan) around the ONH in a rapid succession (1.92 s). Three fast RNFL scans were obtained from each eye in a single session by one operator. The scan circle was centred on the ONH manually. Images with a signal strength (SS) less than 6 were discarded as poor-quality images as recommended by the manufacturer. RNFL thickness was measured using the Stratus OCT system (software version 5.0). Segmentation failure was defined as obvious deviation of the segmented inner and/or outer RNFL borders from the subjectively perceived borders. Consecutive 15% or cumulative 20% segmentation failure within a given image was considered to be of poor analysis quality and discarded.

Cirrus HD-OCT—3D cube OCT data were obtained using the "Optic Disc Cube 200×200 Scan" pattern, which performed raster scanning in a 6×6 mm square centred on the ONH (total scan time was 1.48 s) consisting of 200 frames of horizontal linear B-scans with 200 A-scan lines per B-scan. Images with SS less than 8 were discarded as poor-quality images. This cut-off is different from Stratus SS because, despite both representing signal strength, they are different measurements. There is no validated consensus about the ideal cut-off for Cirrus SS, but the manufacturer recommends that SS 8 or above should be considered acceptable images. In addition to SS, images with detectable eye motion (larger than one vessel diameter or a major distortion of the ONH) in OCT fundus images were also discarded (fig 2B). Analysis quality criteria were the same as Stratus OCT and based on 3.4 mm circular virtual OCT scan images. Three Optic Disc Cube scans were obtained from each eye in a single session by a single operator (KRS).

RNFL thickness measurements

TD-OCT—Global mean, four quadrants, and 12 clock hour RNFL thickness were measured for each of three fast RNFL scans.

SD-OCT—A virtual circular scan with 3.4 mm diameter (256 sampling along the circle) was automatically resampled on each 3D OCT cube data by Cirrus system software after determining the ONH centre. Two methods for determining the ONH centre were employed on Cirrus images:

- Centred Each Time (CET) method. The ONH centre was detected automatically by the Cirrus system separately for each image. RNFL thickness parameters (global, four quadrants and 12 clock hours) were measured along the virtual circle for each

of the three Optic Disc Cube scans (fig 3). This is the method currently implemented in the Cirrus system software.

- Centred Once (CO) method. The ONH centre was automatically detected on the first data cube by the Cirrus system software as described above, then this ONH centre location was imported to the two other data cube sets by registering the OCT fundus image of the first data cube (baseline) to the others (second and third scans). Registration of the OCT fundus images was performed using ImageJ,[13] the public-domain image-processing software for bio-science with TurboReg plug-in (Biomedical Imaging Group, Swiss Federal Institute of Technology, Lausanne, Switzerland) (fig 4).[14] TurboReg registered two given images (baseline against either second or third scans) by performing x, y translation and torsional rotation based on ONH and retinal vessel information. This approach is similar to the ONH analysis method used by HRT. RNFL thickness parameters (global, four quadrants, and 12 clock hours) were then measured along the virtual circle for each of the three Optic Disc Cube scans sharing one universal ONH centre.

Statistical analysis

Linear mixed effect models[15–17] were used to analyse the data from the hierarchical study design and compute the components of variance for the following random effects: subjects, eyes within subjects, eyes within subjects by method interaction and scans within eyes within subjects. The statistical models included both a fixed effect for methods and a random interaction effect between methods and eyes within subjects. The square root of the scan variance component (VC) was computed for each method. Reproducibility is conventionally defined as 2.77 times the square root of the scan variance component. This value represents the difference between two measurements that would be needed in order to have 95% confidence that an observed difference is not due solely to measurement error. Because repeated measurements are taken for each eye of each subject, 95% confidence intervals on the ratios of the reproducibilities for each possible pair of methods had to be computed in order to assess differences in reproducibility between methods. When the ratio between methods is equal to one, the reproducibilities are identical. When the 95% confidence interval does not include one, the reproducibilities for the methods are statistically significant at or below the 5% level of significance. More importantly, the 95% confidence intervals indicate the plausible range of the true ratios of reproducibility and thus indicate how precisely (narrow interval) or imprecisely (wide interval) the ratios are known. The intraclass correlation coefficients (ICCs) were also calculated for each parameter and method using the ratios of the appropriate variance components.

In addition to reproducibility, the distance between ONH centres identified by the CET and CO methods sets was calculated on the second and third 3D OCT scans. Since the centre location is the same for the baseline cube data for CET and CO, baseline cube data were excluded from this analysis.

RESULTS

The mean age of the 14 healthy volunteers (three males and 11 females) was 37.3 (10.3) years. The mean RNFL thickness measurements were 107.5 (9.9) μm (TD-OCT), 97.4 (8.1) μm (SD-OCT: CET) and 97.4 (8.0) μm (SD-OCT: CO) (table 1). There was one instance of algorithm failure, and this scan was excluded from the study. No scan was excluded due to eye motion.

The mean ONH centre location distance between CET and CO was 1.92 (1.63) pixels, which was equivalent to 58 (49) μm on the retina. For global RNFL thickness measurements, the

estimated reproducibility ratio for CET/TD-OCT was 0.370 (95% CI 0.272 to 0.505), which indicates that the reproducibility for CET was better (ie, the variance was smaller) than for TD-OCT (37% of the reproducibility value for TD-OCT). Because the 95% CI does not include one, this indicates that the reproducibilities are statistically significantly different at the 5% level of significance. Similarly, the estimated reproducibility ratios were 0.353 (CI 0.259 to 0.481) for CO/TD-OCT, and 0.953 (CI 0.733 to 1.239) for CET/CO (table 2). For sector RNFL thickness measurements, SD-OCT using CET and CO showed statistically significantly smaller reproducibility ratios than TD-OCT except for 11 o'clock with CET. The reproducibility ratio results imply that, regardless of the ONH centring method, SD-OCT significantly improves RNFL thickness measurement reproducibility (reduces variability) in comparison with conventional TD-OCT. There was no statistically significant difference in reproducibility ratios between CET and CO in any of the global or sectoral measurements.

ICCs for each parameter and method are shown in table 3 along with the corresponding square root of the variance component for scans. ICCs (table 3) from all three methods (TD-OCT, CET and CO) at 11 o'clock were lower than other ICCs. Figure 5 shows that the reproducibility of both CET and CO methods was uniformly and substantially better than TD-OCT, and the differences were statistically significant.

DISCUSSION

The present results showed that the RNFL thickness measurement reproducibility was statistically significantly improved over conventional TD-OCT when using SD-OCT. The acquisition of a 3D data set is likely an important factor in the improvement. The OCT segmentation algorithm takes advantage of the three-dimensional neighbouring structure information available in SD-OCT, which is not possible with a two-dimensional conventional TD-OCT scan, making the SD-OCT segmentation more robust. The higher axial resolution of SD-OCT is a likely contributor as well, as segmentation is more reliable with better-defined RNFL borders.

It is interesting to consider the fact that the scanning time of the SD-OCT 3D cube scan is actually slower than conventional TD-OCT yet achieves a lower RNFL measurement variability. Circular resampling on a 3D cube data requires 56.7% of the 3D data in order to obtain the 3.4 mm circle data (114 out of 200 frames (3.42 mm); each frame vertically covers 30 μm on the retina) that take 0.84 s to acquire, while a single circular scan with TD-OCT takes 0.64 s to acquire. Assuming the characteristics of eye motion during scanning are constant, data acquired using a longer scan time should contain more eye motion artefacts. Nevertheless, SD-OCT showed a lower measurement variability than TD-OCT. This may be because the OCT fundus image provides an easy and reliable way to detect significant eye motion (like a saccade) during a scan so that the eye can be rescanned, if necessary, to minimise eye motion artefacts. With TD-OCT there is no systematic way to detect the magnitude of eye motion during scanning, since the corresponding fundus reference image is captured after the actual OCT scan. It is also possible that the SD-OCT segmentation algorithm is more robust than the TD-OCT algorithm because of a higher axial resolution and readily available 3D structural information as discussed above.

We frequently observed apparent variability in the shape of the automatically detected ONH margins using the Cirrus system software. Because the disc centre was defined based on the location of the disc margin, it was surprising that the CET method did not show a greater variability than the CO method. This is likely because the only information that the virtual circular scan resampling needs is the ONH centre location; it does not take into account ONH shape. Actually, only a 58 μm difference in the ONH centre location was observed

between the CET and CO methods. Gabriele *et al* reported that the peripapillary circular scan has ±350 μm of measurement stability margin where the overall RNFL thickness measurement error stays within the expected measurement error range.[18] The present result of 58 μm ONH centre location deviation is well within this stability margin. Further investigation is needed to see if the same is true on eyes with glaucoma and other pathologies.

In conclusion, SD-OCT 3D cube data provide significantly lower RNFL thickness measurement reproducibility compared with conventional TD-OCT (eg, Stratus OCT). Since the CO method does not have any advantage in measurement reproducibility over the CET method, the RNFL thickness measurement circle placement method employed by the manufacturer is clinically useful.

Acknowledgments

Funding: National Institutes of Health contracts R01-EY13178-09, R01-EY11289-23 and P30-EY08098-20 (Bethesda, Maryland), The Eye and Ear Foundation (Pittsburgh, Pennsylvania) and unrestricted grants from Research to Prevent Blindness (New York).

REFERENCES

1. Schuman JS, Hee MR, Puliafito CA, et al. Quantification of nerve fiber layer thickness in normal and glaucomatous eyes using optical coherence tomography. Arch Ophthalmol 1995;113:586–96. [PubMed: 7748128]
2. Kamal DS, Bunce C, Hitchings RA. Use of the GDx to detect differences in retinal nerve fibre layer thickness between normal, ocular hypertensive and early glaucomatous eyes. Eye 2000;14:367–70. [PubMed: 11027002]
3. Wollstein G, Schuman JS, Price LL, et al. Optical coherence tomography longitudinal evaluation of retinal nerve fiber layer thickness in glaucoma. Arch Ophthalmol 2005;123:464–70. [PubMed: 15824218]
4. Huang D, Swanson EA, Lin CP, et al. Optical coherence tomography. Science 1991;254:1178–81. [PubMed: 1957169]
5. Schuman JS, Hee MR, Arya AV, et al. Optical coherence tomography: a new tool for glaucoma diagnosis. Curr Opin Ophthalmol 1995;6:89–95. [PubMed: 10150863]
6. Ishikawa H, Piette S, Liebmann JM, et al. Detecting the inner and outer borders of the retinal nerve fiber layer using optical coherence tomography. Graefes Arch Clin Exp Ophthalmol 2002;240:362–71. [PubMed: 12073059]
7. Schuman JS, Pedut-Kloizman T, Hertzmark E, et al. Reproducibility of nerve fiber layer thickness measurements using optical coherence tomography. Ophthalmology 1996;103:1889–98. [PubMed: 8942887]
8. de Boer JF, Cense B, Park BH, et al. Improved signal-to-noise ratio in spectral-domain compared with time-domain optical coherence tomography. Opt Lett 2003;28:2067–9. [PubMed: 14587817]
9. Choma MA, Hsu K, Izatt JA. Swept source optical coherence tomography using an all-fiber 1300-nm ring laser source. J Biomed Opt 2005;10:44009. [PubMed: 16178643]
10. Wojtkowski M, Srinivasan V, Fujimoto JG, et al. Three-dimensional retinal imaging with high-speed ultrahigh-resolution optical coherence tomography. Ophthalmology 2005;112:1734–46. [PubMed: 16140383]
11. Nassif N, Cense B, Park BH, et al. In vivo human retinal imaging by ultrahigh-speed spectral domain optical coherence tomography. Opt Lett 2004;29:480–2. [PubMed: 15005199]
12. Wojtkowski M, Bajraszewski T, Gorczynska I, et al. Ophthalmic imaging by spectral optical coherence tomography. Am J Ophthalmol 2004;138:412–19. [PubMed: 15364223]
13. Rasband, WS. ImageJ. 1.39 ed. US National Institutes of Health; Bethesda: 1997–2006.
14. Thévenaz P, Ruttimann UE, Unser M. A pyramid approach to subpixel registration based on intensity. IEEE Trans Image Process 1998;7:27–41. [PubMed: 18267377]

15. Pinheiro, JC.; Bates, DM. Mixed-effects models in S and S-PLUS. Springer; New York: 2000.
16. Demidenko, E. Mixed models: theory and applications. Wiley; Hoboken: 2004.
17. Sahai, H.; Ojeda, MM. Analysis of variance for random models: theory, methods, applications, and data analysis. Vol. Vol. I. Birkhäuser; Boston: 2004.
18. Gabriele ML, Ishikawa H, Wollstein G, et al. Optical coherence tomography scan circle location and mean retinal nerve fiber layer measurement variability. Invest Ophthalmol Vis Sci 2008;49:2315–21. [PubMed: 18515577]

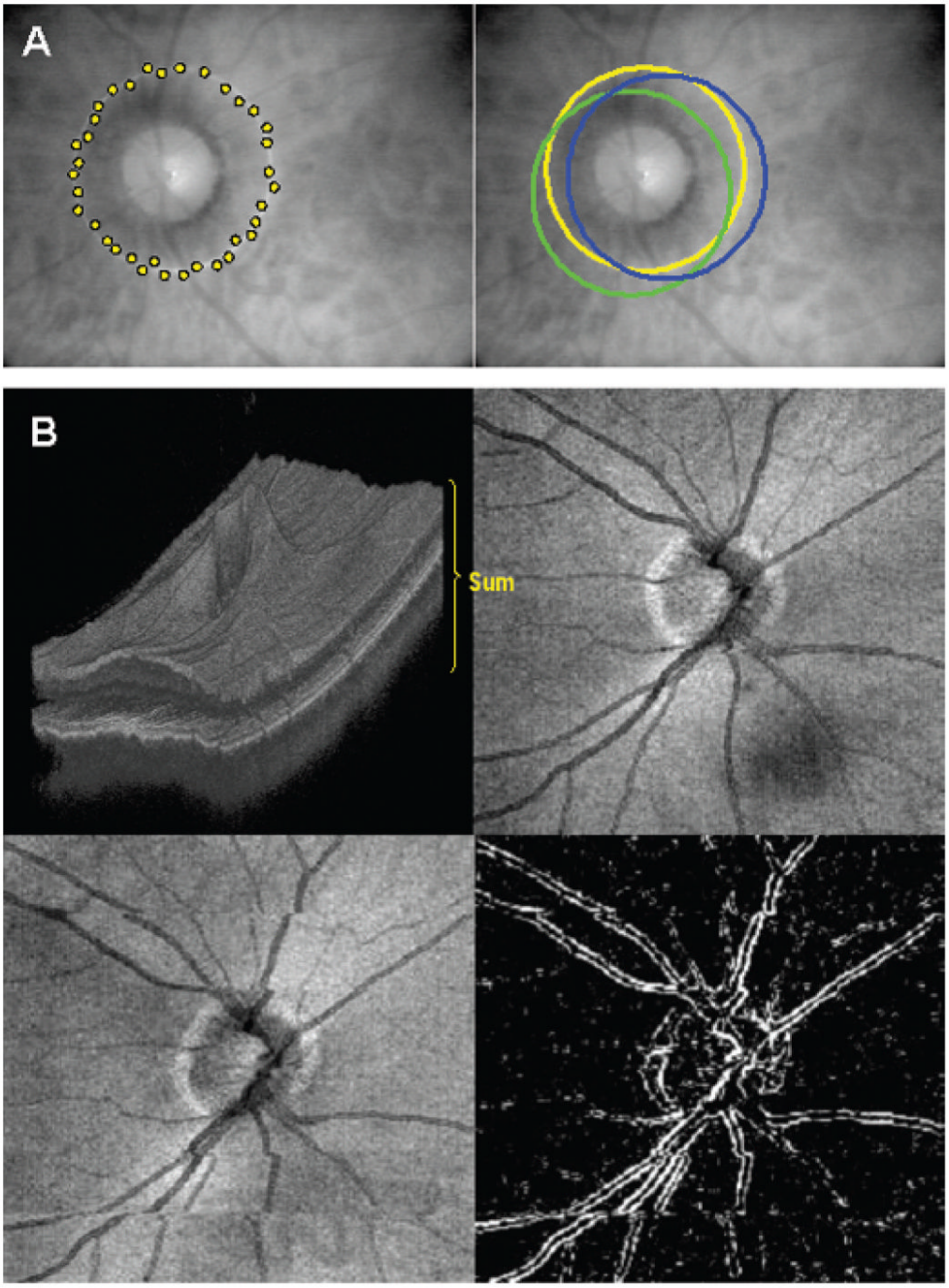

Figure 1.

(A) Major sources of retinal nerve fibre layer thickness measurement variability using 3.4 mm circular time-domain optical coherence tomography scan centred on the optic nerve head. Schematic presentation of sampling points scattered along 3.4 mm diameter circle due to eye motion during the scan (left). Scanning circle placement may vary from scan to scan (right; yellow, green, and blue circles). (B) Spectral-domain optical coherence tomography fundus (en face) image, generated by summing the back scattering signal at each axial scan on the retina. The pseudo-three-dimensional representation on the upper-left shows the direction of summation, and the output image (optical coherence tomography fundus image) is shown on the upper right. Eye motion is detected as disrupted retinal vessels on an optical

coherence tomography fundus image (lower-left), which can be emphasised with edge-detection filtering (lower-right).

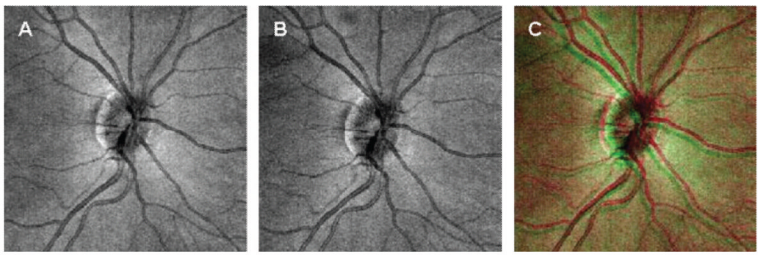

Figure 2.
Two separate optical coherence tomography fundus images (A, B) from the same eye overlaid (C) to emphasise the differences induced by minor eye motion during scanning, head position, and slight shift in the subjects' fixation point. Note that the integrity of retinal vessels within each optical coherence tomography fundus image is intact.

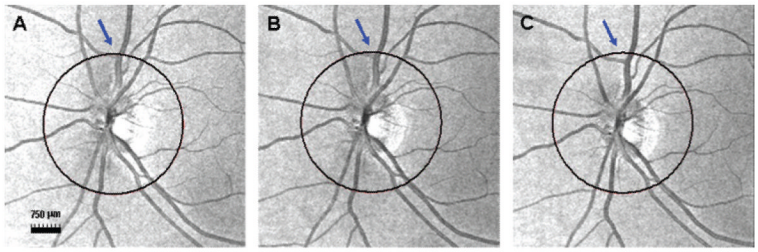

Figure 3.
Centred Each Time method utilising an automatically detected optic nerve head centre on each of the cube data obtained using spectral domain optical coherence tomography. Slight variation in the disc margin detection leads to a displacement of the resampling circle location that can be observed relative to the vessel branches (blue arrow).

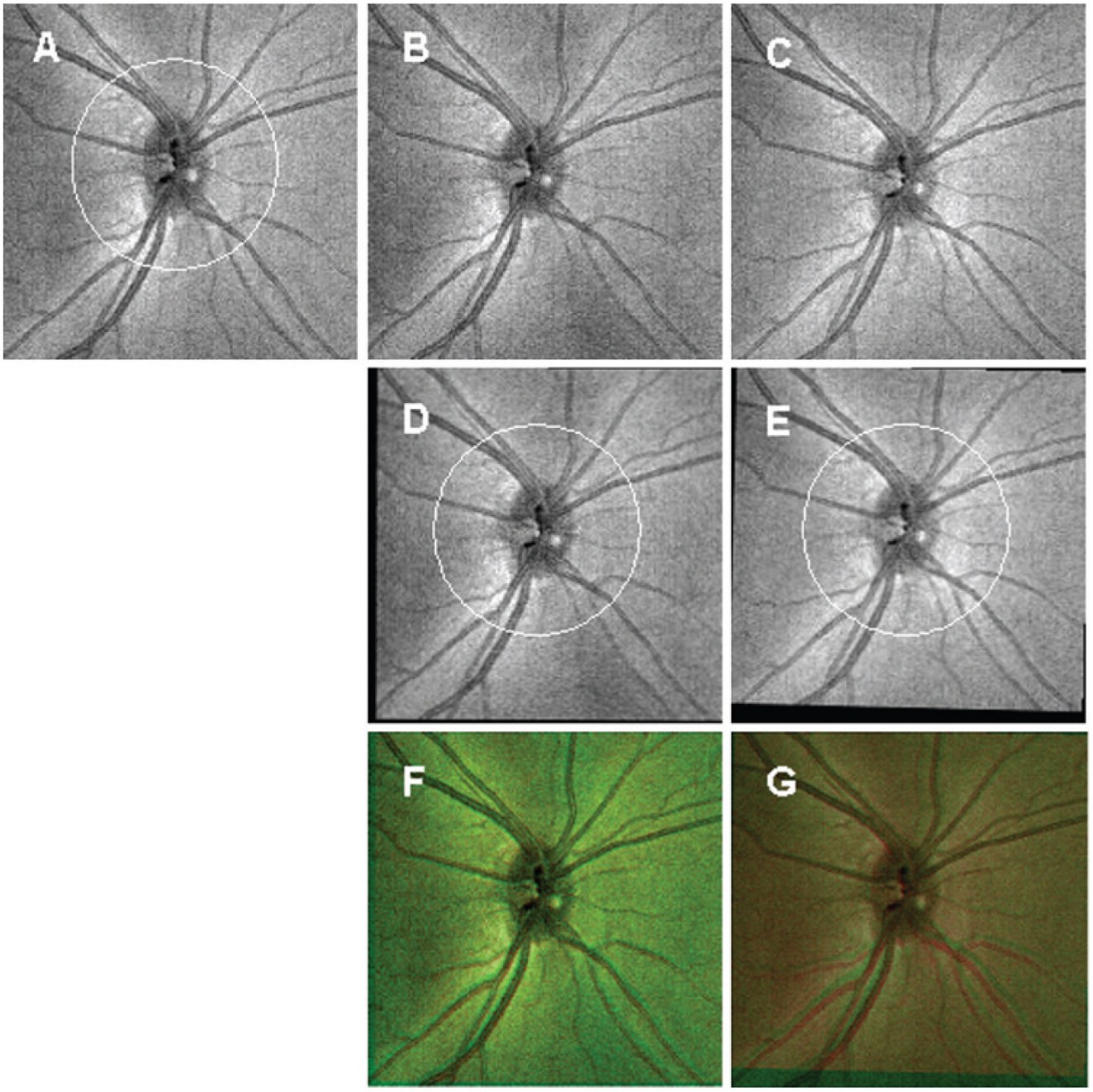

Figure 4.
Centred Once method importing the automatically detected optic nerve head centre from the reference scan (A) onto the other cube data (B and C) obtained from the same eye. Retinal nerve fibre layer thickness measurements were then obtained on each image along the 3.4 mm diameter circle (white circles on (D) and (E)). (F, G) Images visualising the performance of optical coherence tomography fundus image registration by superimposing both the reference image ((A) in red) and the target image ((D) and (E) in green).

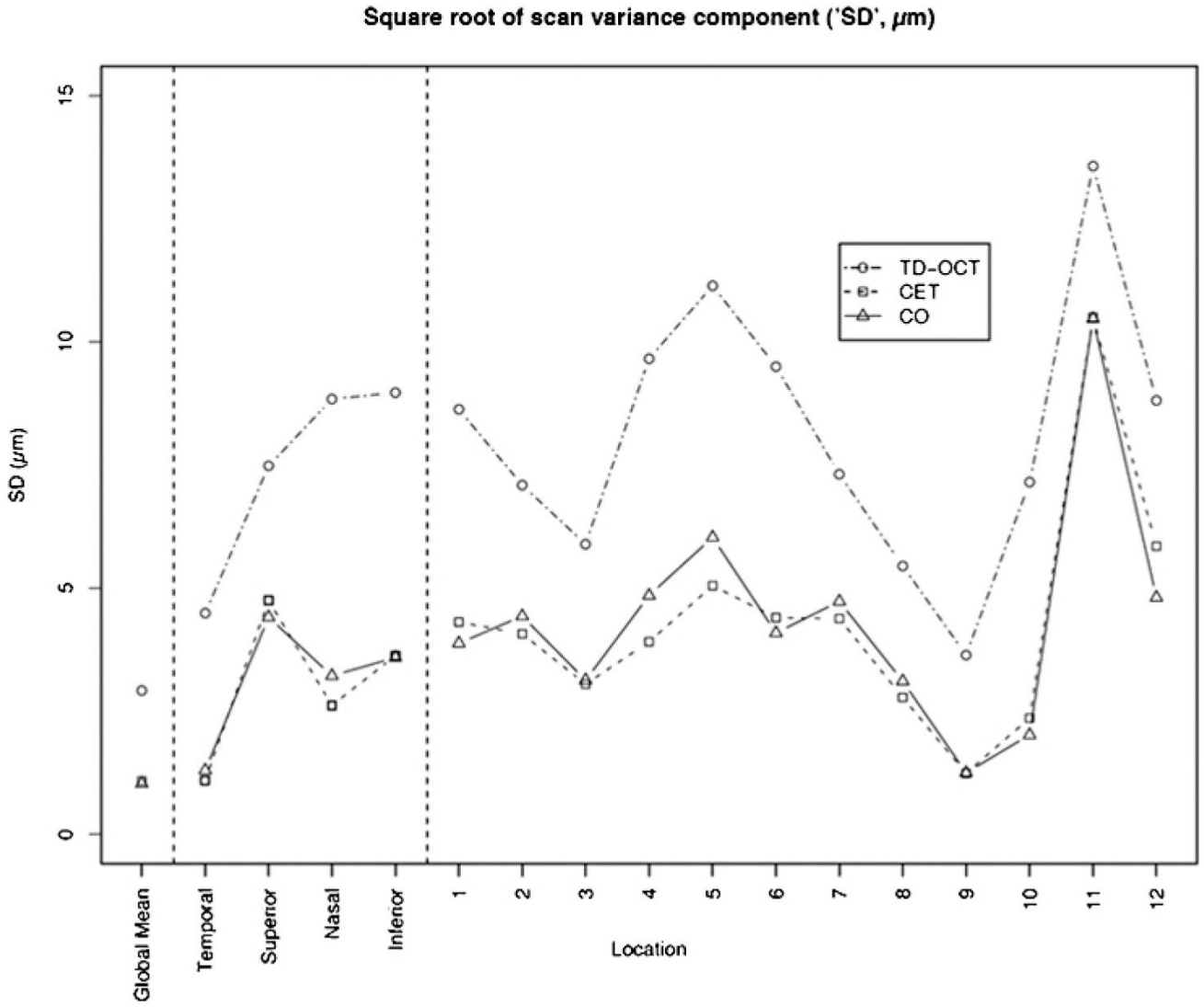

Figure 5.
Square root of scan variance component ("SD") plot from table 3. The reproducibility of both Centred Each Time (CET) and Centred Once (CO) methods was uniformly and substantially better than time-domain optical coherence tomography (TD-OCT) and the differences were statistically significant.

Table 1

Mean (SD) retinal nerve fibre layer thickness measurements of each method

Parameter	Time-domain optical coherence tomography (μm)	Spectral-domain optical coherence tomography	
		Centred Each Time (μm)	Centred Once (μm)
Global mean	107.52 (9.89)	97.42 (8.06)	97.43 (8.01)
Quadrants			
Temporal	80.40 (19.40)	67.07 (11.30)	66.96 (11.38)
Superior	131.24 (10.65)	124.31 (11.05)	125.05 (11.17)
Nasal	80.05 (17.09)	67.95 (13.85)	67.90 (13.52)
Inferior	138.36 (16.41)	130.40 (13.64)	129.65 (13.61)
Clock hour			
1	119.65 (18.28)	111.15 (19.19)	111.91 (19.36)
2	96.73 (26.47)	84.58 (21.93)	84.53 (21.63)
3	65.06 (15.04)	54.41 (10.08)	54.27 (10.05)
4	78.32 (17.37)	64.85 (16.47)	64.89 (16.15)
5	115.01 (21.02)	105.89 (22.41)	105.32 (21.91)
6	146.45 (25.23)	138.41 (23.24)	137.14 (24.17)
7	153.65 (25.91)	146.95 (26.95)	146.54 (27.15)
8	84.42 (22.93)	69.83 (15.55)	70.26 (15.76)
9	61.52 (15.89)	51.38 (8.61)	51.16 (8.59)
10	95.33 (23.71)	79.84 (13.17)	79.49 (13.20)
11	143.35 (21.48)	137.00 (20.35)	137.11 (20.70)
12	130.72 (19.64)	124.78 (21.16)	126.31 (21.64)

Table 2

Reproducibility (variance components) ratios with 95% confidence intervals among the tested methods

	CET vs TD-OCT			CO vs TD-OCT			CET vs CO		
Parameter	**Lower**	**Estimated**	**Upper**	**Lower**	**Estimated**	**Upper**	**Lower**	**Estimated**	**Upper**
Global mean	0.272	0.370	0.505	0.259	0.353	0.481	0.733	0.953	1.239
Quadrants									
Temporal	0.186	0.246	0.325	0.219	0.290	0.384	0.905	1.180	1.540
Superior	0.227	0.287	0.363	0.212	0.269	0.341	0.804	1.008	1.264
Nasal	0.273	0.347	0.441	0.323	0.410	0.522	0.978	1.230	1.545
Inferior	0.429	0.546	0.694	0.448	0.570	0.724	0.771	0.988	1.266
Clock hour									
1	0.402	0.524	0.683	0.354	0.462	0.603	0.716	0.899	1.129
2	0.433	0.574	0.760	0.472	0.625	0.826	0.837	1.089	1.417
3	0.414	0.542	0.709	0.426	0.557	0.728	0.825	1.027	1.277
4	0.423	0.537	0.683	0.440	0.559	0.711	0.986	1.241	1.563
5	0.474	0.602	0.765	0.522	0.663	0.842	0.940	1.195	1.520
6	0.341	0.463	0.630	0.312	0.424	0.576	0.706	0.915	1.186
7	0.451	0.599	0.797	0.488	0.647	0.859	0.828	1.080	1.409
8	0.385	0.509	0.672	0.432	0.570	0.753	0.861	1.120	1.456
9	0.258	0.342	0.453	0.259	0.343	0.455	0.772	1.004	1.306
10	0.247	0.330	0.440	0.211	0.282	0.377	0.656	0.856	1.116
11	0.598	0.774	1.002	0.596	0.771	0.998	0.791	0.997	1.256
12	0.472	0.664	0.935	0.388	0.546	0.767	0.637	0.822	1.060

When a ratio is equal to one, reproducibilities (variance components (VCs)) are identical. Centred Each Time (CET) and Centred Once (CO) methods showed statistically significantly smaller VC ratios than time-domain optical coherence tomography (TD-OCT) except for 11 o'clock with CET. There was no statistically significant difference in reproducibility (VC) ratios between CET and CO.

Table 3

Intraclass correlation coefficients (ICCs), square root of scan variance component (which is approximately the average SD of all eyes) and square root of the scan variance component over the parameter mean for each method for the scans

	ICC			Square root of scan variance component ("SD," μm)			Square root of scan variance component/parameter mean		
Parameter	**TD-OCT**	**CET**	**CO**	**TD-OCT**	**CET**	**CO**	**TD-OCT (%)**	**CET (%)**	**CO (%)**
Global mean	0.894	0.984	0.985	2.92	1.08	1.03	2.7	1.1	1.1
◦ Quadrants									
◦◦ Temporal	0.911	0.994	0.992	4.49	1.10	1.30	5.6	1.6	1.9
◦◦ Superior	0.646	0.742	0.756	7.48	4.75	4.41	5.7	3.8	3.5
◦◦ Nasal	0.696	0.885	0.863	8.84	2.62	3.22	11.0	3.9	4.7
◦◦ Inferior	0.678	0.839	0.840	8.97	3.63	3.59	6.5	2.8	2.8
◦ Clock hour									
◦◦ 1	0.764	0.866	0.878	8.63	4.31	3.88	7.2	3.9	3.5
◦◦ 2	0.915	0.970	0.965	7.09	4.07	4.43	7.3	4.8	5.2
◦◦ 3	0.761	0.860	0.857	5.89	3.05	3.13	9.1	5.6	5.8
◦◦ 4	0.702	0.853	0.824	9.66	3.91	4.85	12.3	6.0	7.5
◦◦ 5	0.712	0.845	0.821	11.14	5.05	6.03	9.7	4.8	5.7
◦◦ 6	0.865	0.968	0.972	9.50	4.40	4.09	6.5	3.2	3.0
◦◦ 7	0.930	0.973	0.969	7.31	4.38	4.73	4.8	3.0	3.2
◦◦ 8	0.917	0.977	0.972	5.45	2.78	3.11	6.5	4.0	4.4
◦◦ 9	0.908	0.988	0.988	3.64	1.24	1.25	5.9	2.4	2.4
◦◦ 10	0.843	0.980	0.985	7.15	2.36	2.02	7.5	3.0	2.5
◦◦ 11	0.629	0.739	0.741	13.57	10.50	10.47	9.5	7.7	7.6
◦◦ 12	0.842	0.924	0.947	8.81	5.85	4.81	6.7	4.7	3.8

Temporal is the lowest random error in all three methods out of quadrants. In absolute terms, nasal and inferior are similar but are reversed in relative terms (square root of scan variance component over parameter mean).

CET, Centred Each Time; CO, Centred Once; TD-OCT, time-domain optical coherence tomography.